Sr/Ca ratios and oxygen isotopes from sclerosponges: Temperature history of the Caribbean mixed layer and thermocline during the Little Ice Age

Alexandra Haase-Schramm,[1] Florian Böhm,[1] Anton Eisenhauer,[1] Wolf-Christian Dullo,[1] Michael M. Joachimski,[2] Bent Hansen,[3] and Joachim Reitner[4]

Received 16 July 2002; revised 12 May 2003; accepted 23 June 2003; published 19 September 2003.

[1] We investigate aragonitic skeletons of the Caribbean sclerosponge *Ceratoporella nicholsoni* from Jamaica, 20 m below sea level (mbsl), and Pedro Bank, 125 mbsl. We use $\delta^{18}O$ and Sr/Ca ratios as temperature proxies to reconstruct the Caribbean mixed layer and thermocline temperature history since 1400 A.D. with a decadal time resolution. Our age models are based on U/Th dating and locating of the radiocarbon bomb spike. The modern temperature difference between the two sites is used to tentatively calibrate the *C. nicholsoni* Sr/Ca thermometer. The resulting calibration points to a temperature sensitivity of Sr/Ca in *C. nicholsoni* aragonite of about −0.1 mmol/mol/K. Our Sr/Ca records reveal a pronounced warming from the early 19th to the late 20th century, both at 20 and 125 mbsl. Two temperature minima in the shallow water record during the late 17th and early 19th century correspond to the Maunder and Dalton sunspot minima, respectively. Another major cooling occurred in the late 16th century and is not correlatable with a sunspot minimum. The temperature contrast between the two sites decreased from the 14th century to a minimum in the late 17th century and subsequently increased to modern values in the early 19th century. This is interpreted as a long-term deepening and subsequent shoaling of the Caribbean thermocline. The major trends of the Sr/Ca records are reproduced in both specimens but hardly reflected in the $\delta^{18}O$ records. *INDEX TERMS:* 1050 Geochemistry: Marine geochemistry (4835, 4850); 3344 Meteorology and Atmospheric Dynamics: Paleoclimatology; 9325 Information Related to Geographic Region: Atlantic Ocean; *KEYWORDS:* Sr/Ca, sclerosponges, oxygen isotopes, Caribbean Sea, Little Ice Age, temperature, thermocline

Citation: Haase-Schramm, A., F. Böhm, A. Eisenhauer, W.-C. Dullo, M. M. Joachimski, B. Hansen, and J. Reitner, Sr/Ca ratios and oxygen isotopes from sclerosponges: Temperature history of the Caribbean mixed layer and thermocline during the Little Ice Age, *Paleoceanography*, *18*(3), 1073, doi:10.1029/2002PA000830, 2003.

1. Introduction

[2] The last ten years of the 20th century probably constitute the warmest decade of the last 1000 years, at least for the Northern Hemisphere [*Mann et al.*, 1999; *Jones et al.*, 2001]. Nevertheless, it is still under debate how much of the observed temperature increase over the last 100 years was caused by anthropogenic climate change and how much is natural variability induced by solar or volcanic forcing, or by multidecadal internal variability of the climate system [*Crowley*, 2000a; *Delworth and Knutson*, 2000; *Stott et al.*, 2000]. Owing to the sparseness of long-term temperature records reaching back to times before human influence on climate became significant, our knowledge of natural climate variations on centennial or millennial timescales is very limited [*Jones et al.*, 2001].

[1]GEOMAR, Forschungszentrum für Marine Geowissenschaften, Kiel, Germany.
[2]Institut für Geologie, Universität Erlangen, Erlangen, Germany.
[3]Institut für Geologie und Dynamik der Lithosphäre, Göttingen, Germany.
[4]Geobiologie, Geowissenschaftliches Zentrum Göttingen, Göttingen, Germany.

0883-8305/03/2002PA000830

[3] Reconstructions of sea surface temperatures from reef coral skeletons on multidecadal, and in some cases even multicentury, timescales [e.g., *Dunbar et al.*, 1994; *Winter et al.*, 2000] are well established in climate research [*Fairbanks et al.*, 1997; *Mann et al.*, 1998; *Evans et al.*, 2000]. However, these corals are restricted to the uppermost few meters of the water column and our knowledge of marine long-term temperature trends is thus largely confined to sea surface temperatures. Only for the last few decades are temperature data from subsurface waters available [*Molinari et al.*, 1997; *Levitus et al.*, 2000; *Vauclair and du Penhoat*, 2001; *Conkright et al.*, 1998].

[4] Multidecadal to millennial-length deeper water (10–200 m) temperature records can be derived from skeletons of sclerosponges [*Swart et al.*, 1998a; *Moore et al.*, 2000]. Sclerosponges build a calcareous skeleton similar to reef corals, but with growth rates one or two orders of magnitude lower, typically less than 0.5 mm per year [*Benavides and Druffel*, 1986; *Reitner and Gautret*, 1996; *Wörheide*, 1998; *Willenz and Hartman*, 1999; *Moore et al.*, 2000; *Böhm et al.*, 2002]. Sclerosponge skeletons lack annual growth bands. Sponge sclerochronologies are therefore usually based on absolute radiometric dating of discrete layers [*Swart et al.*, 1998b; *Wörheide*, 1998; *Moore et al.*, 2000] or on tracer chronologies like stable carbon isotopes,

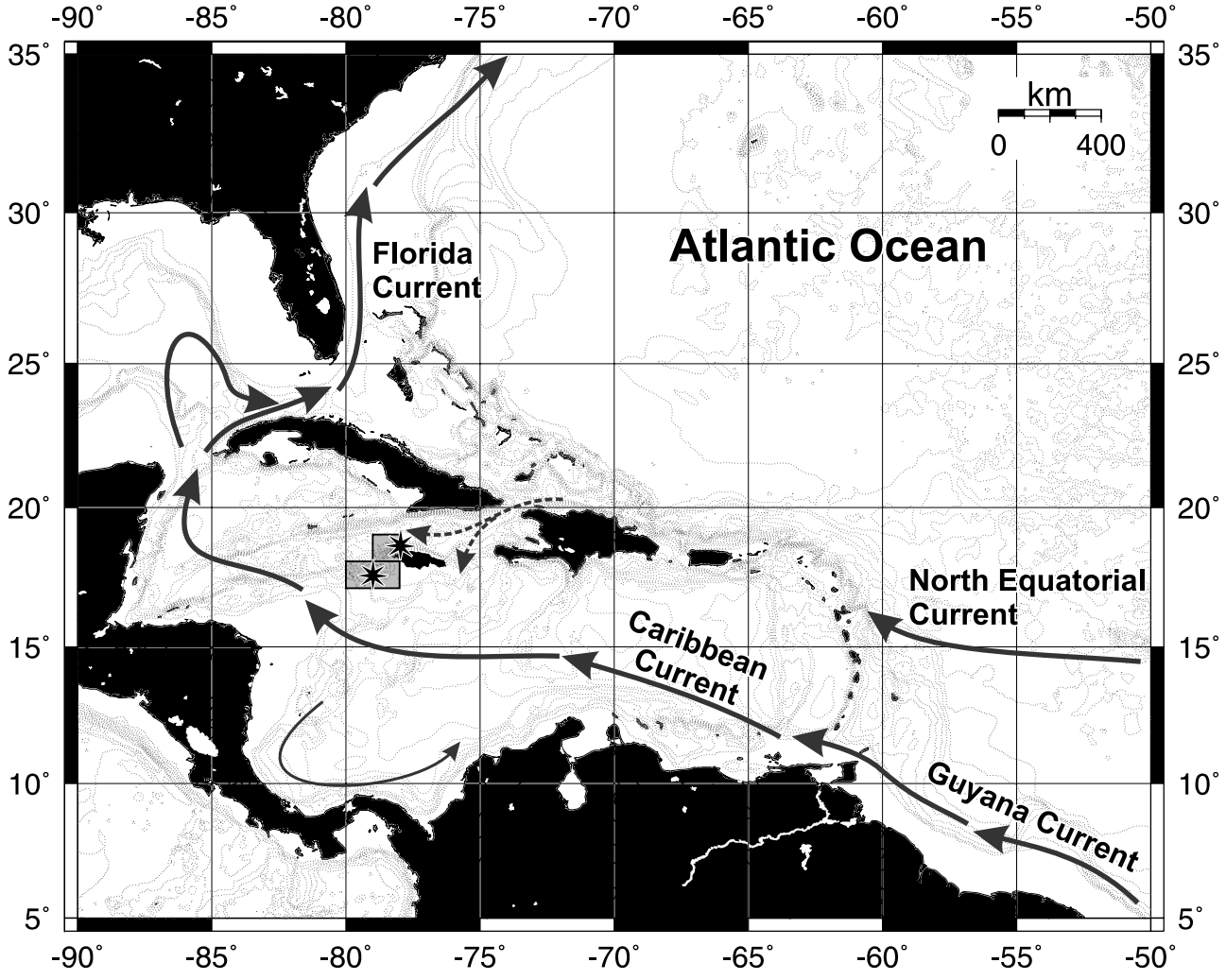

Figure 1. Sampling localities (stars) at Jamaica and Pedro Bank in the Caribbean Sea. Major surface current paths are shown, simplified from *Gordon* [1967], *Schmitz and McCartney* [1993], and *Roberts* [1997]. Grid boxes of the World Ocean Atlas 1998 climatology [*Conkright et al.*, 1998] used in this study are marked by gray squares.

Pb/Ca ratios or the radiocarbon "bomb spike" [*Druffel and Benavides*, 1986; *Joachimski et al.*, 1995; *Böhm et al.*, 1996; *Lazareth et al.*, 2000; *Swart et al.*, 2001].

[5] To date, most sclerosponge-derived temperature reconstructions have been based on oxygen isotopes. Oxygen isotope values measured on several specimens of the Caribbean *Ceratoporella nicholsoni* and the Indopacific *Astrosclera willeyana* agree with expected equilibrium values for local mean temperature and water composition [*Druffel and Benavides*, 1986; *Swart et al.*, 1998a; *Böhm et al.*, 2000a; *Moore et al.*, 2000]. However, despite the apparent isotopic equilibrium, early studies on temperature reconstructions did not yield reproducible trends [*Druffel and Benavides*, 1986; *Joachimski et al.*, 1995; *Wörheide et al.*, 1997; *Böhm et al.*, 1998]. A 700-year oxygen isotope record from a deeper water setting at Lee Stocking Island, Bahamas [*Swart et al.*, 1998b], was the first record showing significant long-term variations, indicating cold periods during the 17th and 18th century and a following warming trend through the 19th and 20th centuries. The first study to successfully compare several oxygen isotope records and interpret reproducible trends was by *Moore et al.* [2000]. They measured oxygen isotopes on up to 100 year old specimens of *A. willeyana* from shallow subsurface water settings (10–20 m) in the Indonesian Seaway. Their sclerosponge records showed different temperature trends than coral records from the same area, indicating a significant subsurface cooling during the last two decades. This was interpreted as evidence for a recent shoaling of the thermocline in this area.

[6] In this study we apply another common temperature proxy, the Sr/Ca ratio of skeletal aragonite. Until recently only few isolated measurements of Sr in sclerosponge skeletons existed [*Veizer and Wendt*, 1976; *Reitner*, 1992]. A first Sr/Ca record of *A. willeyana* measured by *Stewart Fallon* was published in the work of *Swart et al.* [1998b]. Variations in that record pointed to a temperature dependence of the distribution coefficient of Sr/Ca in sclerosponge aragonite. Initial results indicating correlated

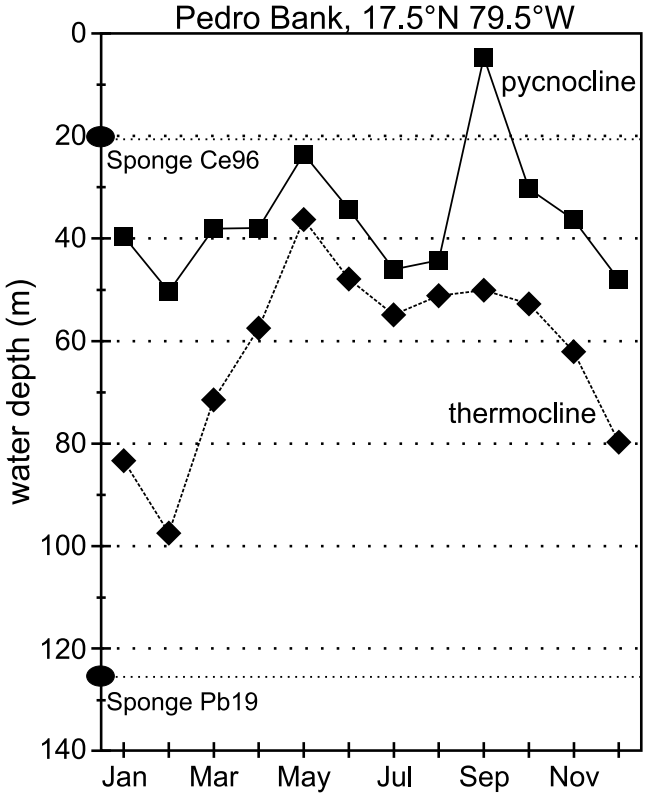

Figure 2. Long-term average monthly position of pycnocline (base of mixed layer) and thermocline in the Caribbean near Pedro Bank. Data from *Levitus and Boyer* [1994] and *Levitus et al.* [1994]. Thermocline depth is the depth where temperature is 0.5 K below sea surface temperature [*Levitus*, 1982]. Pycnocline depth is the depth where density (σ_T) is 0.1 kg/m^3 higher than surface water density. Density calculated according to *Dietrich et al.* [1975]. The depths of the sclerosponge sampling sites are marked by disks on the vertical axis. The Jamaica specimen (Ce96) is projected on the Pedro Bank site, as mixed layer depth is similar at Jamaica and at Pedro Bank.

variations of Sr/Ca and $\delta^{18}O$ in *C. nicholsoni* skeletons, possibly reflecting seasonal temperature changes, were recently described [*Swart et al.*, 2001, 2002a; *Rosenheim et al.*, 2001].

[7] In this paper, we compare Sr/Ca ratios of two specimens of the sclerosponge *C. nicholsoni* that grew at different water temperatures, one in the mixed layer and the other in the upper thermocline, in the northwestern Caribbean. This comparison provides evidence for a pronounced temperature dependence of Sr/Ca ratios in the skeleton of *C. nicholsoni*. We then use the Sr/Ca time series recorded in the sponge skeletons to reconstruct northwestern Caribbean mixed layer and thermocline water temperature variations of the last 600 years.

2. Oceanographic Setting

[8] The uppermost 50–100 m of Caribbean Seawater were termed "Caribbean Surface Water" by *Wüst* [1964]. It forms by the mixing of freshwater from the Amazon and Orinoco Rivers and local sources into tropical Atlantic surface waters, which are then carried to the Caribbean by the Guyana Current (Figure 1). The freshwater influx leads to relatively "low" salinities of about 35.5 to 36 psu [*Morrison and Nowlin*, 1982; *Hernández-Guerra and Joyce*, 2000]. Currently, about 80% of the Caribbean Surface Water has a South Atlantic source while the rest is derived from the North Atlantic [*Schmitz and Richardson*, 1991].

[9] Trade wind-driven coastal upwelling in the southern part of the Caribbean, strongest during winter and early spring, also influences the surface water [*Gordon*, 1967; *Black et al.*, 1999]. The northward shift of the ITCZ during boreal summer with increased rainfall in northern South America and the southern Caribbean leads to augmented riverine input that reaches the northern parts of the Caribbean in late summer and fall [*Hernández-Guerra and Joyce*, 2000]. The interplay of wind and precipitation leads to seasonal variations in the thickness of the mixed layer (Figure 2), with thickness maxima in the northwestern Caribbean in winter and early summer and a pronounced minimum in September, when a thin surface layer of relatively fresh water (35.6 psu in the area of our collection sites) spreads to the northwest [*Levitus et al.*, 1994].

[10] The Caribbean Surface Water is underlain by the Subtropical Underwater [*Wüst*, 1964]. This subsurface water mass forms a salinity maximum (>36.4 psu) at a depth of

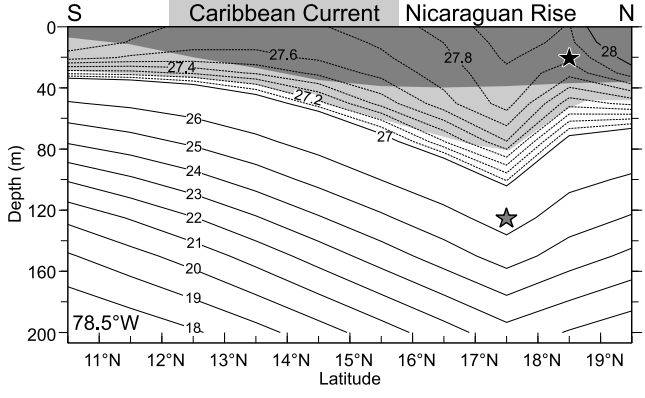

Figure 3. Caribbean annual mean water temperature along a section at 78.5°W [*Conkright et al.*, 1998]. Contour interval is 1 K below and 0.1 K above 27°C, respectively. Isothermal layer (0.5 K criterion) and mixed layer [*Levitus et al.*, 1994] are shown with light and dark shading, respectively. Sponge sampling locations are marked by stars, projected into the plane of the section. The slightly warmer temperature for the 125 m site compared to the value given in the text (section 5.1) results from the strong east-west temperature gradient at the Nicaraguan Rise. The value used in the text is the average of the two grid squares at 17.5°N, 78.5°W (26.4°C) and 17.5°N, 79.5°W (25.6°C). Note shallowing of isothermals in the main flow path of the Caribbean Current (main surface current path from *Fratantoni* [2001] is marked by gray bar) and deepening above the Nicaraguan Rise.

about 150 to 200 m with a temperature of about 23–24°C [*Morrison and Nowlin*, 1982]. These waters are formed mainly during the winter in the eastern part of the tropical-subtropical North Atlantic north of about 20°N from where it sinks along an isopycnal and is advected into the Caribbean [*Morrison and Nowlin*, 1982; *Schmitz and McCartney*, 1993; *Sprintall and Tomczak*, 1992].

[11] The strong salinity gradient between the Caribbean Surface Water and the Subtropical Underwater defines a pycnocline forming the base of the surface mixed layer at about 30 mbsl in the area of our collection sites (Figures 2 and 3). As the Subtropical Underwater derives from relatively warm surface waters, a thermocline is developed below the pycnocline at about 60 mbsl (annual average).

[12] Sea surface and mixed layer temperatures in the Caribbean and tropical North Atlantic are chiefly controlled by the intensity of the northeast trade winds, both through latent heat flux and through Ekman pumping [*Curtis and Hastenrath*, 1995; *Enfield and Mayer*, 1997]. Significant horizontal temperature gradients in the western Caribbean are generated by divergence in the south, deflection of the Caribbean current at the Nicaraguan Rise and convergence south of Jamaica [*Gordon*, 1967] (Figure 3). At a fixed site, variations of wind stress and current intensities can thus create temperature changes on interannual or longer timescales, especially in the deeper water.

[13] The mean seasonal temperature variation in the area of our collection sites is 2.6°C at 20 mbsl and 0.9°C at 125 mbsl (Figure 4). At 125 mbsl the timing of the seasonal extrema is clearly decoupled from the mixed layer and closely follows the seasonal variations at 150 mbsl, that is the core of the Subtropical Underwater [*Levitus and Boyer*, 1994].

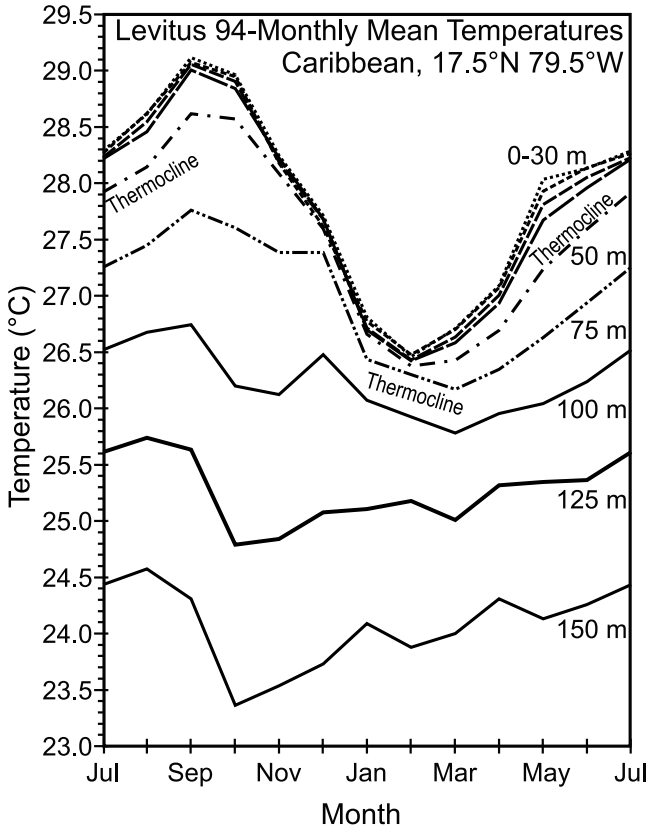

Figure 4. Annual temperature variation at different depth levels at Pedro Bank from *Levitus and Boyer* [1994]. The average position of the thermocline for summer and winter is taken from Figure 2. Mixed layer temperature shows a clear seasonal variation with the minimum around February and the maximum in September. The Subtropical Underwater (depth level 150 m) takes a different seasonal course with a temperature maximum in August and a minimum in October. Temperature at 125 mbsl (specimen Pb19) follows the course of the Subtropical Underwater.

3. Material and Methods

[14] We collected two *Ceratoporella nicholsoni* specimens in the northwestern Caribbean (Figure 1) in spring 1996. One collection site is a reef cave at 20 mbsl at Montego Bay (specimen Ce96), at the north coast of Jamaica (18°28′N, 77°57′W). It is situated in the Caribbean Surface Water and is within the mixed layer during most of the year (Figure 2). The other site is at the NW slope of Pedro Bank (17°32′N, 78°57′W), at 125 mbsl (specimen Pb19), about 200 km southwest from Jamaica. This collection site is situated below the top of the thermocline, in the upper part of the Subtropical Underwater. Both locations are exposed to the open sea.

[15] A radiograph was prepared from a slab of specimen Pb19 cut along the growth axis and milled to a constant thickness of 3 mm. The radiograph was scanned at a resolution of 600 dpi. A densitometric profile was measured on the resulting gray level image with the line profile function of UTHSCSA Image Tool version 2.0.

[16] The porosity of a *C. nicholsoni* skeleton was calculated from measurements of the wet and dry density of a 4 cm long column cut along the growth axis. The resulting value thus represents the average porosity of 0 to about 150 year old skeletal material.

[17] Singular spectrum analysis (SSA) [*Vautard et al.*, 1992] of the oxygen isotope and Sr/Ca records was used to distinguish long-term trends from high-frequency variation and noise with the SSA-MTM toolkit version 4.1 [*Ghil et al.*, 2002]. For the analyses, the records were interpolated to one year time steps. A window of a tenth of the record length was used (i.e., of about 60 years). To test the robustness of the results, all analyses were repeated with half and double window sizes.

[18] We use the double standard deviation (2sd) to indicate the variation of values around a mean. We use the double standard error of the mean ($2sem = 2sd/n^{0.5}$; n = number of measurements) to refer to the 95% confidence interval of a mean value calculated from repeat measurements. Statistical tests (t test, *F* test) were carried out according to *Press et al.* [1989].

3.1. Sr/Ca Ratios and Oxygen Isotopes

[19] About 1–2 mg carbonate powder was collected for Sr- and Ca- ICP-AES analysis using a dental drill with a 0.5 mm diameter drill bit. This corresponds to a temporal resolution of 1–3 years per sample. Sampling was per-

formed parallel to the main growth axis (Figure 5). Carbonate powder was dissolved in 3N HNO_3 and analyzed for Sr and Ca concentrations using an ICP-AES (Yobin Yvon, IY170 ULTRACE). For simultaneous measurements of Sr and Ca, lines at 407.771 nm and 317.933 nm, respectively, were used. The external reproducibility (2sd) of the Sr/Ca ratios was determined to be 1.5% from repeated measurements (n = 123) of the in-house aragonite standard "Ce96-4′." Accuracy was monitored with the international standard "KH." Each sponge sample was measured three times. The average external reproducibility (2sem) determined from these triplicate analyses is 0.6%.

[20] Samples for oxygen isotope analyses were drilled with a 0.5 mm dental drill adjacent to the samples used for Sr/Ca ratios. Offsets between Sr/Ca and oxygen isotope samples were always smaller than 0.2 mm. The drill was operated at the slowest possible drill speed to avoid isotope exchange through heat-induced transformation of the skeletal aragonite [*Aharon*, 1991; *Kuhlmann*, 2000]. Aragonite powders were dissolved with 100% H_3PO_4 at 75°C in an online, automated carbonate reaction device (Kiel Device) connected to a Finnigan Mat 252 mass spectrometer at the University of Erlangen Geological Institute. Isotopic ratios are reported relative to PDB (Peedee belemnite) by assigning a $\delta^{18}O$ value of −2.19‰ (PDB) to standard NBS 19. External precision (2sd) for $\delta^{18}O$ is ±0.07‰ (PDB) based on multiple analyses (n = 87) of standards NBS 19 and IAEA CO1. Temperature-dependent water-aragonite fractionations were calculated based on the equilibrium fractionation equation for aragonite [*Böhm et al.*, 2000a]. The Sr/Ca and oxygen isotope data are available as supplementary material (Appendices A and B) from the World Data Center for Paleoclimatology.[1]

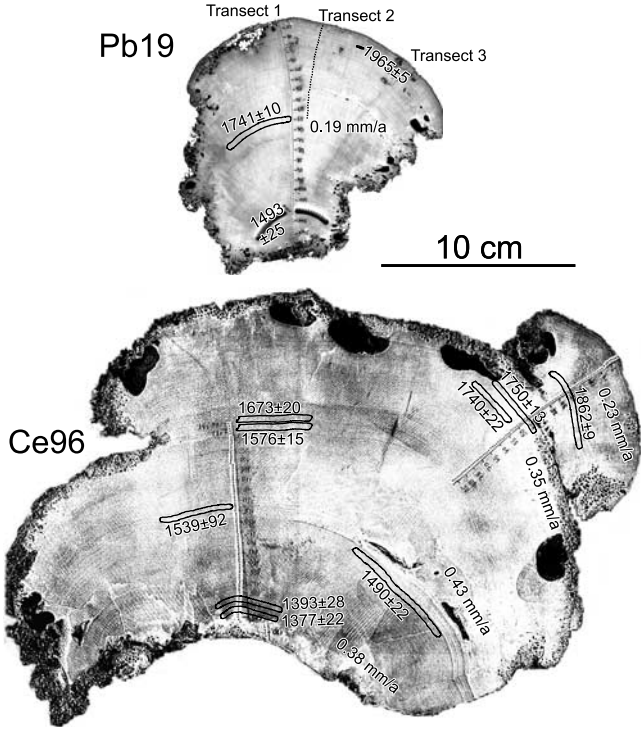

Figure 5. Slabs of the *Ceratoporella nicholsoni* specimens used in this study. Pb19, Pedro Bank, 125 mbsl. Ce96, Jamaica, 20 mbsl. Lines of dots are sampling transects. Three parallel transects were sampled in specimen Pb19. Numbers are years (A.D.) with uncertainties as determined by radiometric dating. Sampling spots of U/Th datings and radiocarbon sample assigned to the year 1965 are marked with bold black lines. Average growth rates (mm/a) were calculated along the sampling transects.

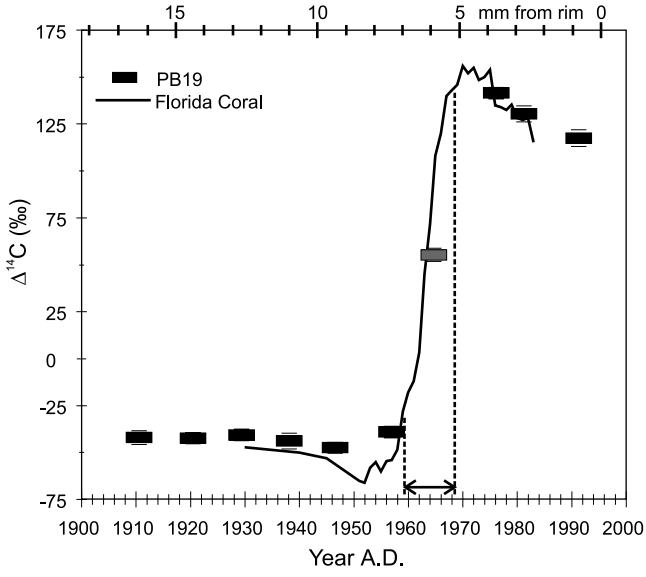

Figure 6. Fit of the measured radiocarbon values to the coral $\Delta^{14}C$ curve for Atlantic Ocean surface waters at Florida [*Druffel*, 1989]. Error bars are smaller than symbols except where shown. The width of the symbols is equivalent to the width of the samples of 1 mm. The upper *x* axis shows the sponge sample distance from the outer rim along the growth axis. We take the position of the sample intermediate between the prebomb and postbomb values to represent the year 1964 ± 5 A.D. in the sponge skeleton. Spacing of the radiocarbon samples is scaled to the lower *x* axis (time) with a growth rate of 0.19 mm/a.

3.2. Age Determination

[21] For U-Th analysis, 0.3 to 1g of sponge material was drilled along visible growth layers. This sample size is a compromise between the analytical requirements for sufficiently large samples and the time comprised in one sample. The sample size was chosen so that the width and depth of the sampling groove was equivalent to a period of about 20 years, given a growth rate on the order of 0.2 mm/a.

[22] The powder was dissolved in warm concentrated HNO_3 and spiked with a ^{229}Th and a ^{233}U-^{236}U double spike. The separation of Th and U was performed similar to the procedures described by *Chen et al.* [1986] and *Edwards et al.* [1987]. Thorium and U were coprecipitated with $Fe(OH)_2$ in alkaline solution (pH 8) using NH_4OH. Uranium and Th were then separated with HBr and HCl, using anion exchange

[1]Supporting appendices are available electronically at World Data Center-A for Paleoclimatology, NOAA/NGDC, 325 Broadway, CO 80303 (e-mail: paleo@noaa.gov; URL: http://www.ngdc.noaa.gov/paleo).

Table 1. Age Data[a]

Sample	Distance From Rim, mm	Width, mm	Age, Years	Year A.D.	Uncertainty, Years 2sem	232Th/230Th Measured	$\delta^{234}U$, ‰	^{238}U, ppm	^{232}Th, ppb	^{230}Th, ppt
Ce96-rim	0	1	0	1996	1	–	–	–	–	–
Ce96-25	34.1	3	135	1862	9	19646	147	7.79	3.64	0.18
Ce96-45	63.8	3	247	1750	13	10787	150	7.71	4.32	0.33
Ce96-51	72.4	4	261	1740	22	6121	155	7.37	2.12	0.33
Ce96-186	111.3	3	327	1673	20	5784	160	7.44	2.54	0.42
Ce96-184	114.9	3	423	1576	15	3966	134	7.29	2.34	0.58
Ce96-123	159.5	3	462	1539	92	3637	161	7.46	2.28	0.60
Ce96-4′	170.0	4	511	1490	22	2544	157	7.44	2.00	0.77
Ce96-151	192.3	4	592	1409	29	2795	162	7.41	2.17	0.76
Ce96-170	215.3	3	608	1393	28	2677	155	7.53	2.16	0.79
Ce96-172	218.0	3	620	1377	22	3484	145	7.84	2.81	0.83
Pb19-rim	0	1	0	1996	1	–	–	–	–	–
Pb19-^{14}C	5.9	1	32	1964	5	–	–	–	–	–
Pb19-64	51.6	3	260	1741	10	7956	159	7.24	2.70	0.33
Pb19-110	99.5	3	505	1493	25	6523	149	7.69	4.48	0.67

[a]For each specimen the first value represents the age of the outermost layer of the skeleton, taken as equal to the sampling year. Sample Pb19-^{14}C is the radiocarbon bomb spike fit described in the text. Distance from rim was measured along the growth axis. Year A.D. is calculated from the age and the year of the measurements (varying from 1997 to 2001 A.D.). Uncertainties of the U-Th dates are internal errors (2 sd) except for sample Ce96-4′. For this sample multiple analyses (n = 5) give an error of about 4% (2sem).

resin Bio Rad AG 1X8 (100–200 mesh) in chloride form. Total blanks are 14 to 30 pg for Th and 13 pg for U. U and Th isotope analyses were carried out on a Finnigan MAT 262 RPQ + mass spectrometer at GEOMAR, Kiel, Germany. Thorium and U were loaded with 1N HNO_3 on an out-gassed Re filament and measured using the double filament technique in the ''peak jumping'' mode. Measurements of the international standard A112 yield a $\delta^{234}U$ of -30.3 ± 6.3‰ (2sd, n = 29). This value is slightly higher but still in accord with the previously reported values of *Edwards et al.* [1993] ($\delta^{234}U$ -34.1 ± 3.4‰, 2sd, n = 6) and *Eisenhauer et al.* [1996] ($\delta^{234}U$ -33.2 ± 4.3‰ , 2sd, n = 11).

[23] For radiocarbon analyses, 10 samples (about 15 mg each) were drilled with a 1 mm dental drill from the uppermost 1.7 cm of skeleton of specimen Pb19. Samples were chemically prepared and measured using the AMS facility at the Leibniz-Labor of the University of Kiel. The aragonite powder samples were cleaned in an ultrasonic bath of 15% H_2O_2 and reacted to graphite using standard procedures [*Nadeau et al.*, 1997]. Conventional radiocarbon ages and $\Delta^{14}C$ values were calculated according to *Stuiver and Polach* [1977]. Precision is better than ±30 conventional radiocarbon years.

[24] We compared our $\Delta^{14}C$ data with a $\Delta^{14}C$ curve measured on a Florida surface water coral [*Druffel*, 1989]. The fit was constrained by assuming that the growth rate was constant in the relevant part of the sponge skeleton. We further assume that the timing of the radiocarbon increase at 125 mbsl was similar to surface waters in that region because the amplitude of change in $\Delta^{14}C$ is similar to the surface water change (Figure 6). The sample position corresponding to the drastic rise in $\Delta^{14}C$, caused by atmospheric nuclear weapon testing, was assigned to the year 1964 A.D.

4. Results

4.1. Chronology

[25] Results of the U and Th analyses are shown in Table 1. The $\delta^{234}U$ ratios, defined as permil deviation of the $^{234}U/^{238}U$ activity ratio from radioactive equilibrium, show values around 154 ± 3‰, which is slightly higher than modern seawater (145 ± 5‰ [*Chen et al.*, 1986]). Individual statistical errors on the U/Th ages vary between 10 and 30 years with one exception of 92 years (Table 1). The external reproducibility of our U/Th dating results was determined as about ±20 years (2sem) by five replicate analyses of sample Ce96-4′ and confirmed by analysis of three closely spaced sample pairs (Ce96-45/51, Ce96-170/172, Ce96-123/4′). For one sample pair (Ce96-184/186) U/Th ages could not be confirmed within external reproducibility.

[26] According to our U/Th dating results, the skeleton of specimen Ce96 represents a time interval from about 1400 A.D. to 1996 A.D. As the age data of this specimen deviate significantly from a linear growth curve, we fitted a third-order polynomial to the U/Th ages (Figure 7). Using the polynomial instead of a linear fit reduces the RMS error by 40% from 37 to 22 years. The latter value is similar to the mean uncertainty of the U/Th data. On the basis of the fitted polynomial, the growth rate of the shallow water sponge specimen Ce96 varied between 0.23 and 0.43 mm/a. For specimen Pb19 a mean growth rate of 0.19 mm/a was calculated from the slope of a linear fit to the dated tie points. A lifespan from about 1400 A.D. to 1996 A.D. was determined by extrapolating the mean growth rate to the base of the skeleton (Figures 5 and 7).

[27] The U/Th chronology is independently confirmed by the correct localization of the nuclear weapon test radiocarbon increase at a depth of about 5.9 mm below the surface of the skeleton (Figure 6, Table 2). Further independent support for the reliability of our chronologies is provided from the fit of $\delta^{13}C$ data of the investigated sponge skeletons and atmospheric CO_2 records [*Böhm et al.*, 2002].

[28] Recently, *Swart et al.* [2002a] postulated short term growth rate variations on the order of 50% in a *C. nicholsoni* skeleton from the Bahamas, based on Sr/Ca ratio variations interpreted to represent annual temperature cyclicity. If this interpretation is correct, such variations could potentially lead to uncertainties of the interpolated ages

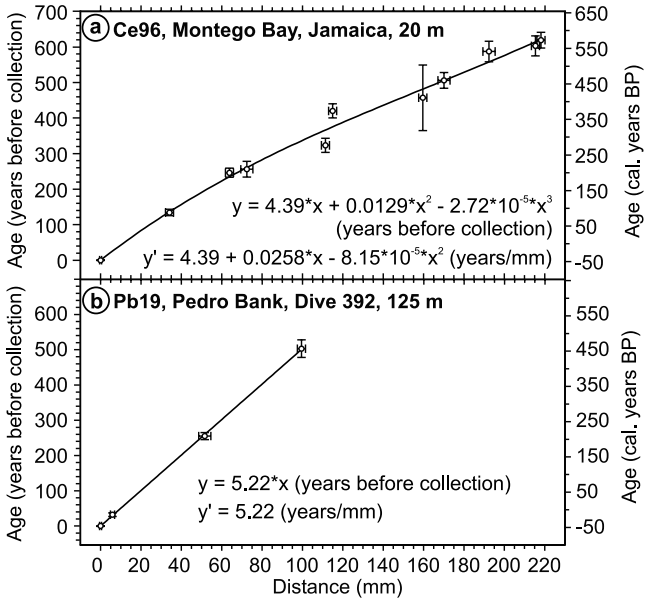

Figure 7. Ages versus depth in skeletons and fitted growth curves. Fit to age data of specimen Ce96 is a third-order polynomial. Age data of Pb19 are fitted by a linear growth model. Left y axes give the year before date of collection (1996 A.D.). Right y axes give the year of formation before present (1950 A.D.). Curve fit equations refer to the years of collection.

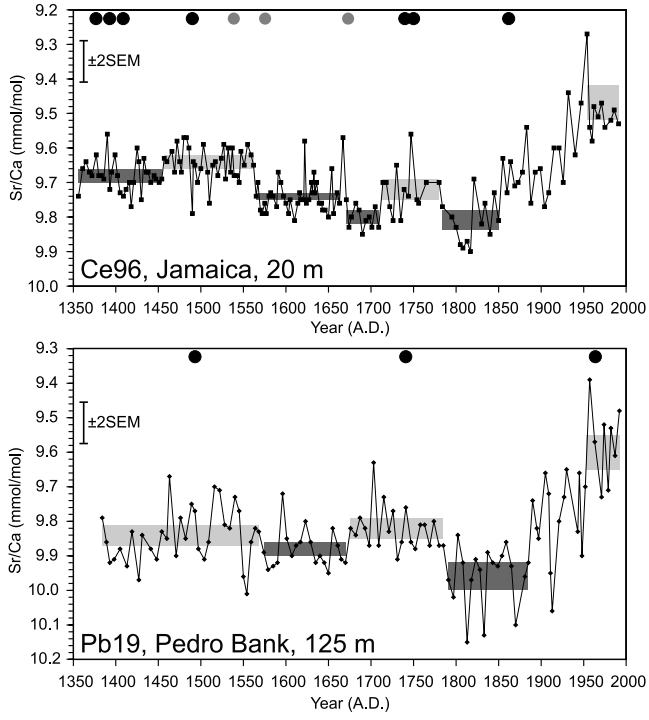

Figure 8. Measured Sr/Ca ratios (small symbols) plotted with the long-term mean values from Table 3 (shaded bars, box height represents ±2sem). Light gray bars refer to warmer (lower Sr/Ca) and dark gray bars to colder (higher Sr/Ca) periods. Sr/Ca scale is plotted inversely. Age tie points are shown as big black dots. Gray dots are uncertain dates (compare to Figure 7).

between our U-Th tiepoints of up to ±25 years. This is within our analytical uncertainties.

[29] In summary, several independent observations support the reliability of our U-Th age dates. The $\delta^{234}U$ values, stratigraphic consistency, reproducibility of repeated measurements and comparison with atmospheric $\delta^{13}C$ and $\Delta^{14}C$ support the chronology of the two sponges.

4.2. Sr/Ca Ratios

[30] The measured Sr/Ca data are presented in Appendix A and Figure 8. Sr/Ca ratios of the shallow water specimen (Ce96) vary between 9.4 and 9.9 mmol/mol, with an average ratio of 9.69 ± 0.01 mmol/mol (2sem). Sr/Ca ratios of the deeper water specimen (Pb19) are generally higher than those of Ce96. The values range from 9.5 to 10.1 mmol/mol with a mean of 9.84 ± 0.02 mmol/mol (2sem). The two record means differ significantly ($p < 0.001$, t test).

[31] Both Sr/Ca data sets were approximated using singular spectrum analysis (SSA) (Figure 9a). Although variations in the Sr/Ca ratios are relatively small compared to analytical errors, they allow the reconstruction of statistically significant long-term trends. For Ce96 the long-term trend is represented by the first two principal components (PC) found by SSA. These explain 62% and 11%, respectively, of the total variance of the Sr/Ca record. For Pb19 the first two PCs, representing the trend, explain 54% and 11%

Table 2. Radiocarbon Data Measured on Specimen Pb19[a]

Sample	Distance From Rim, mm	Corrected Modern Carbon, %	Conventional 14-C Age, Years BP	$\Delta^{14}C$, ‰
Pb19-500	0.8	111.65 ± 0.44	−885 ± 30	117.5 ± 4.4
Pb19-501	2.7	112.81 ± 0.42	−970 ± 30	130.4 ± 4.2
Pb19-502	3.7	113.84 ± 0.31	−1040 ± 20	141.4 ± 3.1
Pb19-503	5.9	105.09 ± 0.35	−400 ± 25	55.2 ± 3.5
Pb19-504	7.4	95.62 ± 0.30	360 ± 25	−39.0 ± 3.0
Pb19-505	9.4	94.70 ± 0.29	435 ± 25	−47.0 ± 2.9
Pb19-506	11.0	94.97 ± 0.42	415 ± 35	−43.3 ± 4.2
Pb19-507	12.7	95.22 ± 0.30	395 ± 25	−39.8 ± 3.0
Pb19-508	14.4	94.97 ± 0.29	415 ± 25	−41.3 ± 2.9
Pb19-509	16.3	94.92 ± 0.36	420 ± 30	−40.7 ± 3.6

[a]Distance from rim is measured along the growth axis. "Percentage of corrected modern carbon" is the fraction of ^{14}C relative to the "modern" value (1950 A.D.), corrected for fractionation using the $^{13}C/^{12}C$ measurements. $\Delta^{14}C$ values were calculated from the corrected percentage of modern carbon using estimates of the true age of the samples taken from the U-Th datings. This age correction is very small (<1% in all samples) so uncertainties introduced by incorrect age estimates are negligible.

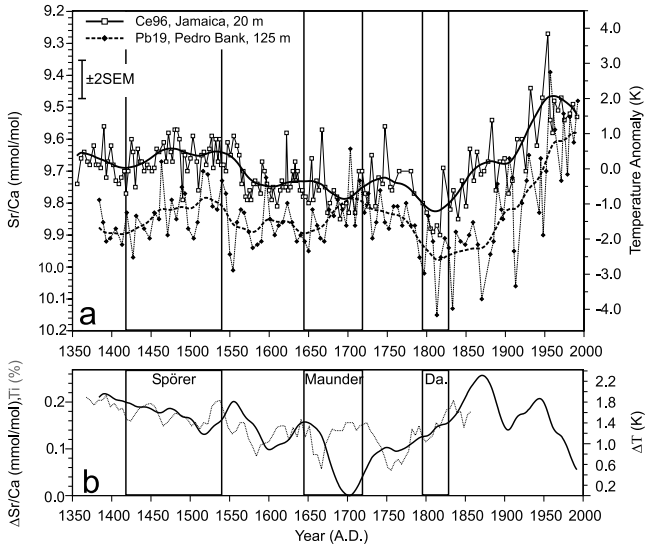

Figure 9. (a) Measured Sr/Ca ratios (small symbols) and long-term trends reconstructed from the first two principal components of SSA (window size 60 years, thick lines). Sr/Ca scale on left *y* axis is plotted inversely. On the right *y* axis estimated temperature anomalies (deviation from Ce96 mean) are shown, according to our Sr/Ca temperature calibration discussed in the text. (b) Difference between the SSA reconstructions of Pb19 and Ce96 (solid line). Note the decreasing difference around 1700 A.D. The right *y* axis shows the calculated corresponding temperature difference. The dotted line is the bulk sediment Ti content from ODP Hole 1002C, Cariaco Basin [*Haug et al.*, 2001a], a proxy for river runoff from northern South America to the southern Caribbean. Low Ti values indicate arid conditions [*Haug et al.*, 2001b]. The durations of the Spörer, Maunder and Dalton (Da.) sunspot minima are shown for comparison.

of the variance, respectively. The third and fourth PC of the Pb19 record represent a weak periodic component with a wavelength of 28 years. Together they explain another 13% of the total variance.

[32] The SSA reconstructed trend curves of both Sr/Ca records show a general increase from low values in the oldest part of the record to a maximum at about 1800 A.D., followed by a general decrease to an absolute minimum in the youngest part of both records. This general trend is overlain by smaller-scale variations (Figure 9a, Table 3). In the shallow water record these are: a relative Sr/Ca maximum in the early 15th century followed by a minor minimum from about 1450 to 1550 A.D., a sharp increase to a maximum after 1550 A.D. and a second, smaller increase in the late 17th century. The time period around 1750 A.D. represents a minor minimum, followed by an increase to the absolute maximum shortly after 1800 A.D. After 1800 A.D., the trend curve falls almost monotonically to the lowest values at about 1950 A.D. Only around 1900 A.D. was this trend briefly interrupted. The trend curve of Pb19 is roughly parallel to the Ce96 trend, except for a short period around 1700 A.D. where the two curves overlap. Through most of the recorded time the offset between the two trend lines varies between 0.2 and 0.1 mmol/mol, with a general decrease from the 14th century until about 1700 A.D. and a subsequent rise in the 18th and 19th centuries (Figure 9b). The offset finally decreases in the late 20th century to about 0.1 mmol/mol.

[33] The maxima and minima seen in the SSA reconstructions are corroborated by comparing the average Sr/Ca ratios of the respective time intervals. All interval means shown in Figure 8 and Table 3 are significantly different from the neighboring intervals (>99% significance level, t test). The only exception is the oldest interval of the Pb19 record with a mean that differs from the mean of the subsequent interval with only 94% significance. In both records the 1950–1992 period mean is significantly lower than any other interval mean.

4.3. Oxygen Isotopes

[34] Oxygen isotope values are listed in Appendix B and shown in Figure 10. Unlike the Sr/Ca records, the shallow and deeper water δ^{18}O curves show no parallel trends. All oxygen isotope ratios of the deeper water sponge (Pb19) are higher than those of the shallow water sponge (Ce96). The difference of the respective mean values is 0.43‰. The mean δ^{18}O for the period 1950–1992 A.D. of the two sponges differs by 0.44 ± 0.05‰, or 1.9 ± 0.3 K (2sem) if converted to temperature with the assumption of a negligible seawater δ^{18}O difference between the sites [*Böhm et al.*, 2000a]. This is in good agreement with the temperature gradient between the two collection sites of 1.8 ± 0.2 K expected from the climatology data [*Conkright et al.*, 1998].

[35] The δ^{18}O of the shallow water specimen (Ce96) varies between −0.95‰ and −0.65‰ (PDB). The overall

Table 3. Average Sr/Ca Ratios for Alternating Periods With High (Boldface) and Low Sr/Ca Means[a]

Ce96, Jamaica, 20 m			Pb19, Pedro Bank, 125 m		
Period	Sr/Ca Mean ± 2SEM (n)	T Test Probability	Period	Sr/Ca Mean ± 2SEM (n)	T Test Probability
1356–1454	9.68 ± 0.02 (31)	0.003	1384–1568	9.84 ± 0.03 (33)	0.060
1457–1562	9.64 ± 0.02 (35)	0.000			
1565–1663	9.74 ± 0.02 (38)	0.000	**1574–1670**	9.88 ± 0.03 (19)	0.003
1671–1709	9.80 ± 0.02 (11)	0.001			
1714–1780	9.72 ± 0.04 (13)	0.001	1676–1785	9.82 ± 0.03 (21)	0.000
1784–1850	9.81 ± 0.04 (13)	0.000	**1791–1885**	9.96 ± 0.04 (18)	0.000
1954–1991	9.49 ± 0.05 (10)		1952–1992	9.60 ± 0.05 (9)	

[a]The mean values are given with standard error intervals (sem = standard deviation/$n^{0.5}$) and the number of measurements (n) for each time period. The t test significance values give the probability that the mean value of the respective time interval is equal to the mean of the subsequent interval. The means for the 1950–1990 period are weighted, taking account for the individual confidence intervals (2sem) of the measured values.

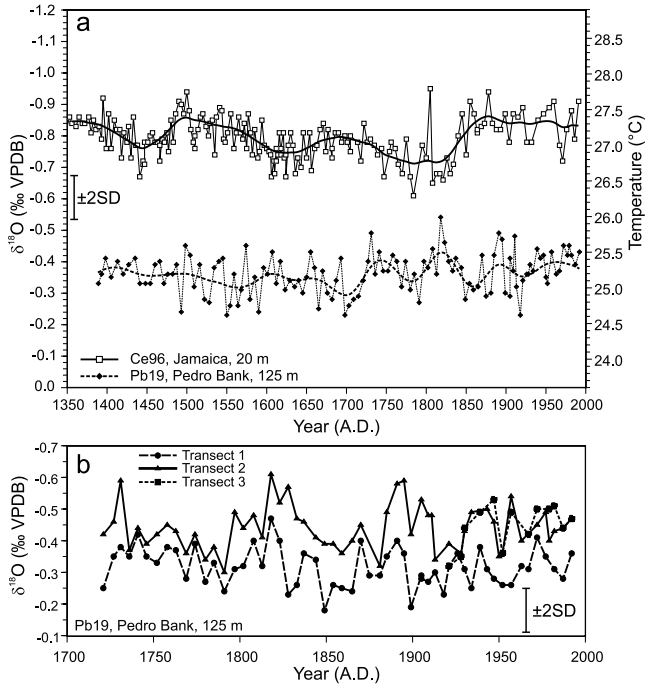

Figure 10. Oxygen isotope data. (a) Shallow and deeper water record. Thick lines are reconstructions from the first two principal components of SSA (window size 60 years). The older part of the Pb19 record is from transect 1, the younger part is a stack of the three transects shown in Figure 10b. Temperatures on the right *y* axis are calculated for a constant $\delta^{18}O_{water}$ of 0.8‰ (SMOW) applying the temperature equation of *Böhm et al.* [2000a]. (b) Three transects through specimen Pb19. For position of the transects compare Figure 5.

mean is −0.79 ± 0.01‰, the mean for the 1950–1991 A.D. period is −0.84 ± 0.05‰ (2sem). The first two PCs found by SSA explain 44% and 12% of the variance, respectively. The 3rd and 4th PC constitute an oscillatory component with a periodicity of 40 years and together represent 14% of the total variance. The reconstruction from PCs 1 and 2 is shown in Figure 10a.

[36] In the deeper water sponge (Pb19), $\delta^{18}O$ varies between −0.25‰ and −0.55‰ with an overall mean of −0.36 ± 0.01‰ and a 1950–1992 A.D. mean of −0.40 ± 0.03‰ (2sem). Three transects were sampled as a test for reproducibility (Figures 5 and 10b). Correlation between the transects was carried out by following the growth bands of the skeleton. The trends and larger features are well-reproduced in the three transects. However, transect 1 is offset from the other two transects by about 0.1‰. For the subsequent discussion we therefore use a stacked record, averaging the three transects (Figure 10a).

[37] SSA of the stacked record of Pb19 does not produce the clear trend components as the other records. The first two PCs explain only 19% and 17% of the total variance, respectively. The 3rd and 4th PC, like in the shallow water record, constitute an oscillatory component with a periodicity of about 40 years. Together the latter explain 24% of the total variance. The reconstruction from the first two PCs (Figure 10a) reveals multidecadal variations, most prominent during the last 300 years, superimposed on a very weak long-term trend.

5. Discussion

5.1. Temperature Calibration of Sr/Ca Ratios

[38] So far no temperature calibration is available for Sr/Ca ratios in sclerosponge skeletons. In order to translate the observed Sr/Ca variations into temperatures, we use the contrast in water temperature and skeletal Sr/Ca ratios between the shallow and the deeper water site to establish a preliminary Sr/Ca temperature calibration for *Ceratoporella nicholsoni*. Annual mean water temperature averaged over the last 50 years is 27.8 ± 0.2°C (±2sem) at 20 mbsl for the 1°*1° grid square centered at 18.5°N, 78.5°W (west of Jamaica) and 26.0 ± 0.2°C at 125 mbsl for the two grid squares centered at 17.5°N, 78.5°W and 79.5°W (east and west of the Pedro Bank sampling site, Figure 1) [*Conkright et al.*, 1998]. This corresponds to a temperature difference of 1.8 ± 0.2 K between the two locations. The average temperature difference for the same time interval calculated from our measured $\delta^{18}O$ values is 1.9 ± 0.3 K.

[39] The average Sr/Ca ratios for the 1950 to 1991 A.D. period are 9.47 ± 0.05 mmol/mol (shallow water, Ce96) and 9.60 ± 0.05 mmol/mol (deeper water, Pb19), respectively (Table 3). From the difference between these two average values of −0.13 ± 0.07 mmol/mol and the temperature difference of 1.8 ± 0.2 K, a Sr/Ca temperature relation of −0.07 ± 0.04 mmol/mol/K is calculated.

[40] Comparison with other marine aragonitic material shows that the temperature control of Sr/Ca variation of *C. nicholsoni* (−0.07 ± 0.04 mmol/mol/K) is similar to reef corals (−0.05 to −0.08 mmol/mol/K [*De Villiers et al.*, 1994; *Shen et al.*, 1996; *Swart et al.*, 2002b]) but slightly stronger than in inorganic aragonite (−0.04 mmol/mol/K [*Kinsman and Holland*, 1969]).

[41] Applying the Sr/Ca temperature calibration (−0.07 ± 0.04 mmol/mol/K) to the sponge records we find a temperature change between the periods with the highest and the lowest Sr/Ca ratios (Table 3) of about 5 K (3–12 K, 95% confidence interval). We realize that temperature variations of up to 12 K are unrealistic for the Caribbean, compared to the maximum tropical Atlantic Ocean cooling of less than 5 K during the last glacial maximum [*Crowley*, 2000b]. Thus we realize that realistic temperature variations are only found by using the calibration value at the lower limit of the 95% confidence interval (−0.11 mmol/mol/K), resulting in minimal temperature change.

[42] Regional variations of the seawater Sr/Ca ratio, variable calcification rates and precipitation of secondary cement in skeletal pores may complicate and obscure the application of the Sr/Ca temperature proxy. However, for our case we can largely exclude such complications as discussed in the following.

5.1.1. Influences From Sr/Ca Variations in the Seawater

[43] *De Villiers* [1999] showed an increase of Sr/Ca ratios from 8.49 mmol/mol at the surface to 8.57 mmol/mol at 100 m in the equatorial central Atlantic. A shallow-deep water difference of this magnitude would change the scle-

rosponge Sr/Ca thermometer to −0.03 mmol/mol/K. The latter value results in unrealistically large temperature amplitudes of more than 10 K. The deeper water sponge (Pb19) is situated in the transition zone between the Caribbean Surface Water and the Subtropical Underwater. Subtropical Underwater originates from the tropical-subtropical North Atlantic. This water generally carries higher Sr/Ca ratios than the waters originating in the South Atlantic [*De Villiers*, 1999], which are the main sources for the Caribbean Surface Water. Thus Pb19 may be enriched in Sr/Ca in contrast to sample Ce96, resulting in a possible effect similar to the one discussed above.

[44] Varying Sr/Ca in the surface water due to local runoff could add some uncertainty to the calibration. Diagenetic alteration and chemical weathering of elevated Plio-/Pleistocene coral reefs along the northern coast of Jamaica could be a Sr source for coastal waters at Montego Bay (Ce96). However, our Jamaican sponge grew in a reef cave exposed to the open ocean, where the effect of local Sr input can be considered to be negligible.

5.1.2. Influences of Calcification Rate and Secondary Cementation

[45] Various studies have discussed the possible influence of calcification rates on the Sr/Ca ratios of coral skeletons [*De Villiers et al.*, 1994]. *Zhong and Mucci* [1989] found rate-independent Sr/Ca ratios for inorganic aragonite, precipitated with rates of up to 230 μmol/m^2/h, and possibly up to 660 μmol/m^2/h as indicated by a single data point. Reef corals, on the other hand, show much higher calcification rates with typical values for *Porites* around 20,000 ± 10,000 μmol/m^2/h [*De Villiers et al.*, 1994; *Lough and Barnes*, 1997]. We estimate calcification rates for *C. nicholsoni* from the measured extension rates (0.2–0.4 mm/a), porosity (~4%) and noncarbonate contents (organic carbon and opaline needles, ~4%). This results in values ranging from 500 to 1400 μmol/m^2/h, about an order of magnitude lower than reef coral calcification rates.

[46] *De Villiers et al.* [1994] suggested that reef corals incorporate less Sr in their skeletons ($D_{Sr} = (Sr/Ca)_{coral}/(Sr/Ca)_{seawater} \approx 1.0$ at 27°C) than inorganically precipitated aragonite ($D_{Sr} \approx 1.1$ at 27°C [*Kinsman and Holland*, 1969]) because of their high calcification rates. From the mean Sr/Ca ratios for tropical Atlantic surface waters [*De Villiers*, 1999] and the mean Sr/Ca ratio of specimen Ce96 for the period 1950–1991 A.D., we estimate $D_{Sr} \approx 1.1$ (27°C) for the aragonite of *C. nicholsoni*. This is in good agreement with the value for inorganic precipitates.

[47] If calcification rate would influence the Sr uptake of *C. nicholsoni* like in reef corals, then the older, fast growing portion of specimen Ce96 (growth rate 0.4 mm/a) would be depleted in Sr compared to the slow growing young part (0.2 mm/a). This would mean that the actual temperature increase from the 17th century to modern times would be even larger than calculated from the measured Sr/Ca ratios.

[48] It has been shown that precipitation of secondary aragonite can distort the Sr/Ca signal in reef corals [*Müller et al.*, 2001; *Enmar et al.*, 2000]. If this were also valid for our sclerosponges, the roughly 0.3 mmol/mol increase from the youngest to older skeletal parts could be due to a gradual addition of secondary cement with a higher Sr/Ca ratio than the primary aragonite. The necessary amount of secondary aragonite can be calculated in a simple mass balance:

$$x_s = \left((Sr/Ca)_b - (Sr/Ca)_p\right) / \left((Sr/Ca)_s - (Sr/Ca)_p\right)$$

where x_s is the percentage of secondary cement in the bulk material and subscripts b, p, and s stand for bulk, primary and secondary, respectively. We assume a Sr/Ca ratio of about 9.5 mmol/mol for the pristine skeletal material (Table 3) and of 10.5 mmol/mol for the secondary cement [*Kinsman and Holland*, 1969; *Enmar et al.*, 2000]. To achieve the observed 0.3 mmol/mol increase in Sr/Ca, one has to add nearly half as much cement as there is primary aragonite. As shown in the radiograph in Figure 11, there is no porosity decrease across the zone of Sr increase (top 20 mm in Pb19, top 40 mm in Ce96). We have measured the bulk porosity of *C. nicholsoni* skeletons as less than 5%. A porosity decrease from about 40% below the living surface to 5% in the older skeleton would be easily visible in the radiograph. The only porosity change visible in Figure 11 takes place in the outermost 5 mm, which is not compatible with the observed Sr trend that covers the youngest 20 mm. We therefore exclude the presence of a significant secondary aragonite phase in our sponge skeletons.

[49] We conclude that neither secondary cementation nor calcification rate variations significantly influenced our Sr/

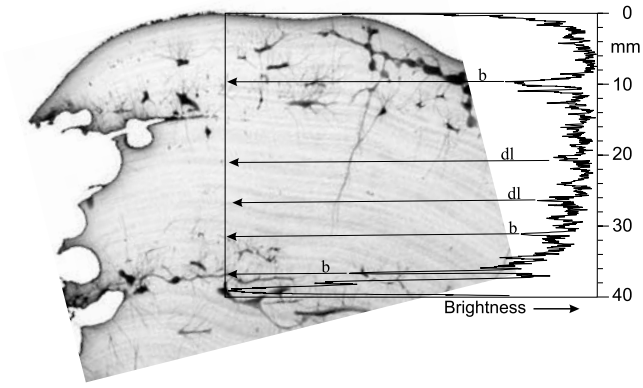

Figure 11. Radiograph of specimen Pb19 indicating porosity of the skeleton. The upper rim of the skeleton (dark lining) is the growth surface, which is covered by soft tissue. Note dark sponge borings ("b") and faint dark laminations ("dl") in the radiograph. The curve shows the image brightness measured along a 0.5 mm wide profile positioned at the left rim of the black rectangle. Lower brightness indicates lower density/higher porosity. The curve shows increasing brightness values (decreasing porosity) in a roughly 5 mm thick layer below the dark growth surface. Further inside the skeleton, brightness shows fluctuations between bright and dark layers, but no further trends, except for the bored zone at the base of the profile.

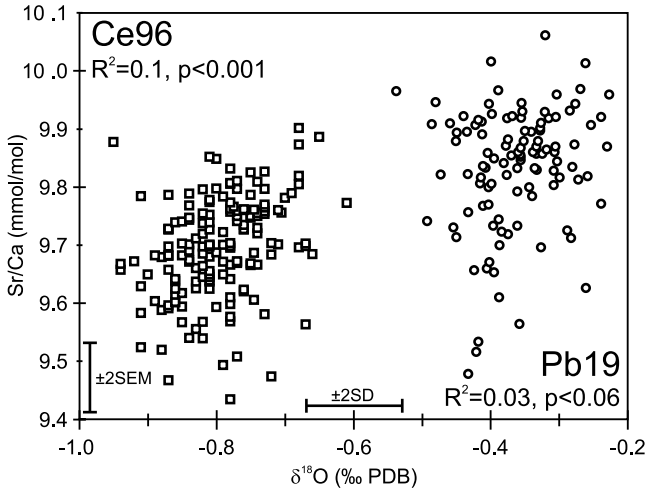

Figure 12. Scatterplot of the measured Sr/Ca ratios and the corresponding oxygen isotope values. Correlation is highly significant for Ce96. However, $\delta^{18}O$ and Sr/Ca share only 10% of common variance.

Ca records. Seawater Sr/Ca contrasts between the two sampling sites cannot be excluded, but their contribution to the Sr/Ca temperature calibration would be to increase the amplitudes in the sponge temperature records to unrealistically high values.

5.2. Comparison of Sr/Ca and $\delta^{18}O$

[50] Samples for Sr/Ca and $\delta^{18}O$ were taken from the same growth layers immediately adjacent to each other. This allows us to directly compare both parameters from each sample pair. Linear regression of the measured Sr/Ca ratios on the $\delta^{18}O$ values shows a weak but significant correlation ($R^2 = 0.1$, $p < 0.001$) for specimen Ce96. Variability of $\delta^{18}O$ explains 10% of the Sr/Ca variability. The correlation for specimen Pb19 is not significant ($p < 0.06$) (Figure 12).

[51] The smoothed $\delta^{18}O$ and Sr/Ca curves (Figure 13a) of the shallow water record both display a temperature minimum at about 1800 A.D. and a subsequent temperature rise until the late 19th century. However, while the Sr/Ca temperatures continue to rise, the $\delta^{18}O$ temperatures show no further increase. Moreover, the amplitudes of the $\delta^{18}O$ variations are much smaller than expected for the temperature variations derived from the Sr/Ca record. The deeper water oxygen isotope record does not reflect any of the long-term trends seen in the Sr/Ca record (Figure 13b).

[52] The assumption that the Sr/Ca record of *C. nicholsoni* aragonite is primarily controlled by temperature implies that the $\delta^{18}O$ records must be strongly controlled by other factors as well. Certainly part of the 90% independent variability of both proxies is introduced by the low signal/noise ratios. Additional $\delta^{18}O$ variability could originate from salinity variations. The $\delta^{18}O_{water}$ salinity relation in the Caribbean is on the order of 0.2 to 0.3‰/psu [*Rühlemann et al.*, 1999; *Watanabe et al.*, 2001]. The long-term temperature variations of 3 K derived from the Sr/Ca ratios are equivalent to $\delta^{18}O$ variations of 0.7‰, about twice as much as observed (Figure 12). Salinity variations of up to 2 psu could compensate for no more than 0.6‰ of $\delta^{18}O$. Larger salinity changes are unlikely for the Caribbean.

[53] The pH-dependent fractionation of oxygen isotopes in carbonates may further influence the $\delta^{18}O$ of the sponge skeletons. The $\delta^{18}O$ of carbonates precipitated in a pH range of 6 to 9 decreases by about 1.5‰ per pH unit [*Zeebe*, 1999]. Thus variations of 0.5 pH units in the fluid from which the skeletal aragonite is precipitated can account for the observed oxygen isotope variability. The observation that sponges precipitate aragonite in chemical and isotopic equilibrium indicates that the composition of the precipitating fluid is hardly influenced by the sponge metabolism. Thus pH changes in the ambient seawater may be directly monitored by the $\delta^{18}O$ record of the sponge aragonite. This hypothesis is supported by the boron isotopic composition of sponge skeletons, which indicates mineralization under seawater pH conditions [*Böhm et al.*, 2000b]. So, other than for corals, which through symbiont and metabolic activities strongly control their precipitating fluid pH [*McConnaughey et al.*, 1997; *Hemming et al.*, 1998], the $\delta^{18}O$ of sponge skeletons could be strongly influenced by seawater pH changes. Measurements from the Pedro Bank area at water depths of 125 ± 25 mbsl taken in 1972 and 1973 show an average pH of 8.2 with variations of about ±0.2 (NODC Oceanographic Profile Database, www.nodc.

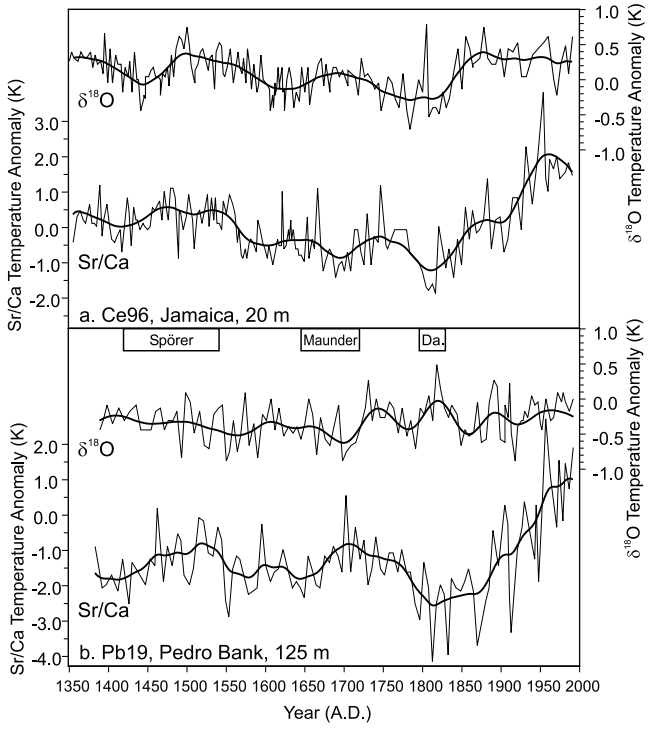

Figure 13. Comparison of the temperature anomaly estimates (deviation from Ce96 mean) based on Sr/Ca ratios (left y axes, temperature calibration as discussed in the text) and oxygen isotope values (right y axes, temperature equation from *Böhm et al.* [2000a]). The durations of the Spörer, Maunder and Dalton (Da.) sunspot minima are shown for comparison.

noaa.gov/JOPI/). Thus seawater pH variability could add about 0.6‰ of temperature-independent $\delta^{18}O$ variability. We conclude that, together with variations in seawater $\delta^{18}O$, the pH effect on $\delta^{18}O$ of carbonates can obscure the temperature signal in the sponge $\delta^{18}O$ record sufficiently to explain the divergent trends of the Sr/Ca and the oxygen isotope records. These results indicate that for temperature reconstructions using *C. nicholsoni* skeletons, Sr/Ca is a more robust proxy than $\delta^{18}O$.

5.3. Temperature History

[54] Our preliminary Sr/Ca temperature calibration of *C. nicholsoni* skeletons shows that the observed record of Sr/Ca variations can be used to draw conclusions about the long-term Caribbean temperature history. Applying our "minimum calibration" (−0.11 mmol/mol/K) to the measured Sr/Ca records, we estimate long-term temperature variations to be on the order of 3 K, both at Jamaica, 20 mbsl, and at Pedro Bank, 125 mbsl (Figure 9a).

[55] Both sponges record the coldest temperatures of the last 600 years at the beginning of the 19th century (Figure 9a). The temperature difference between the shallow and deeper water site was significant most of the time, except for an interval between 1650 and 1700 A.D., when the two records became statistically indistinguishable (Table 3, Figure 9). During this interval the shallow water cooled while the deeper water warmed. The absence of a significant temperature gradient means that the base of the isothermal layer deepened to a level below the Pb19 site.

[56] As shown in Figure 9b, the temperature difference between the two sponge collection sites follows a similar long-term trend as the Titanium content of sediments from the Cariaco Basin in the southern Caribbean [*Haug et al.*, 2001a]. The latter has been interpreted as a proxy for river runoff from northern South America to the southern Caribbean [*Haug et al.*, 2001b]. The decreasing trend of Ti from the 14th century until about 1750 A.D. is paralleled by the decreasing shallow-deep temperature contrast of our sponge records. Lower Ti values point to less freshwater input to the Caribbean Surface Water and at the same time to an increased upwelling of Subtropical Underwater in the southern Caribbean [*Haug et al.*, 2001b; *Black et al.*, 1999]. Both would lead to a salinity increase in the Caribbean Surface Waters and with that to a reduced density contrast between the surface and the Subtropical Underwater. This in turn would favor the deepening of the thermocline observed to occur between the 14th and 17th centuries (Figure 9b). A return to more humid conditions in the southern Caribbean after 1750 A.D., reflected in increasing Ti values, allowed the re-establishment of the stable salinity induced density stratification as it exists in the Caribbean today, and led to a rise of the thermocline to its modern level.

[57] There are no long-term temperature records available from the Caribbean or western tropical Atlantic that would allow a direct comparison with our sclerosponge reconstructions. Closest to our data is the multiproxy reconstruction of tropical North Atlantic temperatures [*Mann et al.*, 1998; *Waple et al.*, 2002]. For the pre-1850 A.D. period it is mainly based on tree ring data from the North American continent. No Atlantic or Caribbean marine temperature proxy records were used. This land-based reconstruction shows two cold periods in the late 17th and in the early 19th century that agree with our reconstructed shallow water temperature trend, and also with the early 19th century minimum being colder than the late 17th century minimum. However, it must be noted that the magnitudes of the coolings are two to three times smaller in the reconstruction than implied by our Sr/Ca record, if we apply our preliminary sclerosponge calibration to quantify the temperature variations.

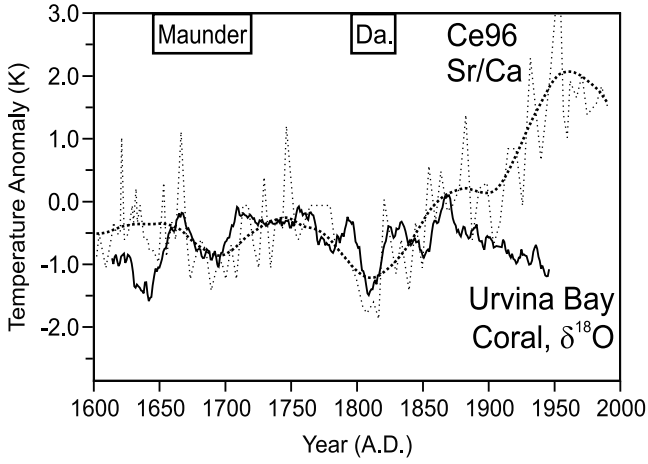

Figure 14. Comparison of the temperature anomalies calculated from the shallow water Sr/Ca record (dotted lines) and a coral $\delta^{18}O$ SST reconstruction from Urvina Bay, Galapagos (solid line) [*Dunbar et al.*, 1994]. The annual coral data are smoothed with a 15 year running average. The durations of the Maunder and Dalton (Da.) sunspot minima are shown for comparison.

[58] An annually resolved coral SST reconstruction from the east Pacific Ocean (Urvina Bay, Galapagos [*Dunbar et al.*, 1994]) shows similar trends as our shallow water temperature record between 1650 and 1850 A.D. (Figure 14). Similar to our Caribbean record, the late 17th and the early 19th century are cold intervals.

[59] Climate model experiments [*Shindell et al.*, 2001; *Waple et al.*, 2002] have shown that these two cold intervals can be explained by reduced solar irradiation during the "Maunder" and "Dalton" sunspot minima, respectively. In contrast to the cold periods of the late 17th and early 19th century, the cooling around 1550 A.D., indicated by our records, does not correlate with known variations of solar irradiance (Figure 9a).

[60] Our preliminary Sr/Ca temperature calibration does not yet allow us to precisely quantify the warming from the Little Ice Age to modern temperatures. However, a comparison of the magnitude of change in Sr/Ca ratios during the last 200 years with the fluctuations during the preceding centuries clearly points to the exceptional nature of this recent warming in the Caribbean Sea (Figure 9).

[61] Most published tropical ocean temperature records indicate a late 20th century that is 1–2 K warmer than the Little Ice Age [*Crowley and North*, 1991; *Keigwin*, 1996;

Corrège et al., 2001; *Müller et al.*, 2002]. A stronger warming on the order of 2–3 K from 1780–85 A.D. to the present was found in a coral record of sea surface temperatures from Puerto Rico, northeastern Caribbean [*Winter et al.*, 2000; *Watanabe et al.*, 2001]. *DeMenocal et al.* [2000] found a 3–4 K warming of sea surface temperatures in the subtropical North Atlantic off West Africa from about 1650 A.D. to modern times using planktonic foraminiferal assemblage census counts with a temporal resolution of 50–100 years.

[62] The strong warming since the early 19th century reflected in our Sr/Ca records is not seen in the observational (1856–1991 A.D.) Caribbean SST anomaly time series of *Kaplan et al.* [1998]. Correlation of our Sr/Ca records and the SSTA data (averaged to a triannual resolution) results in correlation coefficients of −0.4 (Pb19, $n = 27$, $p < 0.02$) and −0.3 (Ce96, $n = 27$, $p < 0.08$). These weak correlations indicate a decoupling of the water temperatures at both sponge collection sites from local SST at the interannual timescale resolved by our data. This is not surprising for the deeper water site which is positioned below the thermocline (Figure 2) at a water depth clearly decoupled today from seasonal SST variations (Figure 4). At our shallow water (20 m) site the relatively sheltered cave setting may have provided for some decoupling from the surface environment. A similar decoupling of shallow water (10–20 m) temperatures from SST on interannual to decadal timescales was also described from the Indonesian Seaway by *Moore et al.* [2000].

[63] The decoupling from SSTs suggests that temperatures at both sites are mainly controlled by subsurface advection of water. The large horizontal temperature gradients found in the Caribbean (Figure 3) allow for the advection of waters of different temperatures to any one location just by modifying the wind field or the strength and flow path of the Caribbean current. Therefore the large amplitude temperature variations seen in both of the subsurface sponge records but not in Caribbean SST records may be explained by advection of waters with varying temperatures, possibly in connection with changes in the thermohaline circulation.

6. Summary and Conclusions

[64] Sr/Ca ratios of *Ceratoporella nicholsoni* skeletons are a sensitive and reliable temperature proxy, superior to $\delta^{18}O$. Oxygen isotope records of these sponges do not reveal reproducible temperature signals. Variations in the $\delta^{18}O$ of the ambient water and the pH effect on the oxygen isotopic composition of carbonates [*Zeebe*, 1999] may obscure temperature signals in the $\delta^{18}O$ records.

[65] Caribbean water temperatures warmed significantly from the early 19th century until the late 20th century, both at the shallow and the deeper water site. Neither of our sponge records represents sea surface temperatures. Even at 20 mbsl the temperature trend is decoupled from local SST. Subsurface advection likely controls the water temperatures. The two cold periods during the late 17th and the early 19th century recorded by the shallow water sponge coincide with the Maunder and Dalton sunspot minima, respectively, and were probably caused by solar forcing. Water temperatures were cooler during these periods compared to the preceding centuries. The major initial cooling step, however, had occurred already by the late 16th century, after the end of the Spörer minimum, and cannot be explained by solar forcing.

[66] The long-term decrease of the temperature contrast between the two sclerosponge sites from the 14th to the late 17th century reflects the aridification of the southern Caribbean during the Little Ice Age [*Haug et al.*, 2001b]. We propose that the position of the thermocline, reflected by this temperature contrast, was controlled on multidecadal timescales by the salinity gradient between the Caribbean Surface Water and the Subtropical Underwater and by wind driven mixing and upwelling.

[67] **Acknowledgments.** Financial support to AHS and AE was provided by the "Deutsche Forschungsgemeinschaft" (Ei272/10-1). We thank Pieter Grootes, Leibniz-Labor Kiel, for providing radiocarbon measurements. Anja Müller and Amos Winter are thanked for hints and discussions, as is Kristina Kuhlmann for discussions and help with laboratory work. Many thanks to Helmut Lehnert for collecting and providing the Caribbean sclerosponge skeletons. The critical reviews of Andrea Grottoli, an anonymous referee, and the editor Larry Peterson are gratefully acknowledged.

References

Aharon, P., Recorders of reef environment histories: Stable isotopes in corals, giant clams, and calcareous algae, *Coral Reefs*, *10*, 71–90, 1991.

Benavides, L. M., and E. Druffel, Sclerosponge growth rate as determined by ^{210}Pb and $\Delta^{14}C$ chronologies, *Coral Reefs*, *4*, 221–224, 1986.

Black, D. E., L. C. Peterson, J. T. Overpeck, A. Kaplan, M. E. Evans, and M. Kashgarian, Eight centuries of North Atlantic Ocean atmosphere variability, *Science*, *286*, 1709–1713, 1999.

Böhm, F., M. M. Joachimski, H. Lehnert, G. Morgenroth, W. Kretschmer, J. Vacelet, and W.-C. Dullo, Carbon isotope records from extant Caribbean and South Pacific sponges: Evolution of $\delta^{13}C$ in surface water DIC, *Earth Planet. Sci Lett.*, *139*, 291–303, 1996.

Böhm, F., M. M. Joachimski, A. Eisenhauer, H. Lehnert, W.-C. Dullo, G. Wörheide, and J. Reitner, Coralline sponges as palaeoclimate recorders, paper presented at European Meeting of the International Society for Reef Studies, Ecole Pratique des Hautes Etudes, Univ. de Perpignan, Perpignan, France, 1998.

Böhm, F., M. M. Joachimski, W.-C. Dullo, A. Eisenhauer, H. Lehnert, J. Reitner, and G. Wörheide, Oxygen isotope fractionation in marine aragonite of coralline sponges, *Geochim. Cosmochim. Acta*, *64*, 1695–1703, 2000a.

Böhm, F., A. Deyhle, A. Eisenhauer, and W.-C. Dullo, Anthropogenic pH decline of Caribbean surface waters reflected in boron from sclerosponge skeletons, *Eos Trans. AGU*, *81*(48), Fall Meet. Suppl., Abstract OS11B-13, 2000b.

Böhm, F., A. Haase-Schramm, A. Eisenhauer, W.-C. Dullo, M. M. Joachimski, H. Lehnert, and J. Reitner, Evidence for preindustrial variations in the marine surface water carbonate system from coralline sponges, *Geochem. Geophys. Geosys.*, *3*(3), doi:10.1029/2001GC000264, 2002.

Chen, J. H., R. L. Edwards, and G. J. Wasserburg, ^{238}U, ^{234}U and ^{232}Th in seawater, *Earth Planet. Sci. Lett.*, *80*, 241–251, 1986.

Conkright, M., S. Levitus, T. O'Brien, T. Boyer, J. Antonov, and C. Stephens, *World Ocean Atlas 1998 Data Set Documentation* [CD-ROM], *Tech. Rep. 15, NODC Internal Rep.*, Nat. Oceanogr. Data Cent., 1998.

Corrège, T., T. Quinn, T. Delcroix, F. Le Cornec, J. Récy, and G. Cabioch, Little Ice Age sea surface temperature variability in the southwest tropical Pacific, *Geophys. Res. Lett.*, *28*, 3477–3480, 2001.

Crowley, T. J., Causes of climate change over the past 1000 years, *Science*, *289*, 270–277, 2000a.

Crowley, T. J., CLIMAP SST re-revisited, *Clim. Dyn.*, *16*, 241–255, 2000b.

Crowley, T. J., and G. R. North, *Paleoclimatology*, *Oxford Monogr. Geol. Geophys*., vol. 18, 349 pp., Oxford Univ. Press, New York, 1991.

Curtis, S., and S. Hastenrath, Forcing of anomalous sea surface temperature evolution in the tropical Atlantic during Pacific warm events, *J. Geophys. Res.*, *100*, 15,835–15,847, 1995.

Delworth, T. L., and T. R. Knutson, Simulation of early 20th century global warming, *Science*, *287*, 2246–2250, 2000.

DeMenocal, P., J. Ortiz, T. Guilderson, and M. Sarnthein, Coherent high- and low-latitude climate variability during the Holocene warm period, *Science*, *288*, 2198–2202, 2000.

De Villiers, S., Seawater strontium and Sr/Ca variability in the Atlantic and Pacific oceans, *Earth Planet. Sci. Lett.*, *171*, 623–634, 1999.

De Villiers, S., G. T. Shen, and B. K. Nelson, The Sr/Ca-temperature relationship in coralline aragonite: Influence of variability in $(Sr/Ca)_{seawater}$ and skeletal growth parameters, *Geochim. Cosmochim. Acta*, *58*, 197–208, 1994.

Dietrich, G., K. Kalle, W. Krauss, and G. Siedler, *Allgemeine Meereskunde*, Borntraeger, Berlin, 1975.

Druffel, E. M., Decade timescale variability of ventilation in the North Atlantic: High precision measurements of bomb radiocarbon in banded corals, *J. Geophys. Res.*, *94*, 3271–3285, 1989.

Druffel, E. M., and L. M. Benavides, Input of excess CO_2 to the surface ocean based on $^{13}C/^{12}C$ ratios in a banded Jamaican sclerosponge, *Nature*, *321*, 58–61, 1986.

Dunbar, R. B., G. M. Wellington, M. W. Colgan, and P. W. Glynn, Eastern Pacific sea surface temperature since 1600 A.D.: The $\delta^{18}O$ record of climate variability in Galapagos corals, *Paleoceanography*, *9*, 291–315, 1994.

Edwards, R. L., J. H. Chen, T. L. Ku, and G. J. Wasserburg, Precise timing of the last interglacial period from mass spectrometric determination of thorium-230 in corals, *Science*, *236*, 1547–1553, 1987.

Edwards, R. L., J. W. Beck, G. S. Burr, D. J. Donahue, J. M. A. Chappell, A. L. Bloom, E. R. M. Druffel, and F. W. Taylor, A large drop in atmospheric $^{14}C/^{12}C$ and reduced melting in the Younger Dryas, documented with ^{230}Th ages of corals, *Science*, *260*, 962–968, 1993.

Eisenhauer, A., Z. R. Zhu, L. B. Collins, K. H. Wyrwoll, and R. Eichstätter, The last interglacial sea level change: New evidence from the Abrolhos islands, West Australia, *Geol. Rundschau*, *85*, 606–614, 1996.

Enfield, D. B., and D. A. Mayer, Tropical Atlantic sea surface temperature variability and its relation to El Nino-Southern Oscillation, *J. Geophys. Res.*, *102*(C1), 929–945, 1997.

Enmar, R., M. Stein, M. Bar-Matthews, E. Sass, A. Katz, and B. Lazar, Diagenesis in live corals from the Gulf of Aqaba: I. The effect on paleo-oceanography tracers, *Geochim. Cosmochim. Acta*, *64*, 3123–3132, 2000.

Evans, M. N., A. Kaplan, and M. E. Cane, Intercomparison of coral oxygen isotope data and historical sea surface temperature (SST): Potential for coral-based SST field reconstructions, *Paleoceanography*, *15*, 551–563, 2000.

Fairbanks, R. G., M. N. Evans, J. L. Rubenstone, R. A. Mortlock, K. Broad, M. D. Moore, and C. D. Charles, Evaluating climate indices and their geochemical proxies measured in corals, *Coral Reefs*, *16*, S93–S100, suppl., 1997.

Fratantoni, D. M., North Atlantic surface circulation during the 1990s observed with satellite-tracked drifters, *J. Geophys. Res.*, *106*(C10), 22,067–22,093, 2001.

Ghil, M., M. R. Allen, M. D. Dettinger, K. Ide, D. Kondrashov, M. E. Mann, A. W. Robertson, A. Saunders, Y. Tian, F. Varadi, and P. Yiou, Advanced spectral methods for climatic time series, *Rev. Geophys.*, *40*(1), 1003, doi:10.1029/2000RG000092, 2002.

Gordon, A. L., Circulation of the Caribbean Sea, *J. Geophys. Res.*, *72*, 6207–6223, 1967.

Haug, G. H., K. A. Hughen, L. C. Peterson, D. M. Sigman, and U. Röhl, Cariaco Basin trace metal data, *Data Contrib. Ser., 2001-071*, World Data Cent. A for Paleoclimatol., Boulder, Colo., 2001a. (Available at http://www.ngdc.noaa.gov/paleo/data.html.)

Haug, G. H., K. A. Hughen, L. C. Peterson, D. M. Sigman, and U. Röhl, Southward migration of the Intertropical Convergence Zone through the Holocene, *Science*, *293*, 1304–1308, 2001b.

Hemming, N. G., T. P. Guilderson, and R. G. Fairbanks, Seasonal variations in the boron isotopic composition of coral: A productivity signal?, *Global Biogeochem. Cycles*, *12*, 581–586, 1998.

Hernández-Guerra, A., and T. M. Joyce, Water masses and circulation in the surface layers of the Caribbean at 66°W, *Geophys. Res. Lett.*, *27*, 3497–3500, 2000.

Joachimski, M. M., F. Böhm, and H. Lehnert, Long-term isotopic trends from Caribbean demosponges: Evidence for isotopic disequilibrium between surface waters and atmosphere, in *Coral Reefs in the Past, Present and Future*, vol. 29, edited by B. Lathuiliere and J. Geister, pp.141–147, Serv. Géol. du Luxembourg, Luxembourg, 1995.

Jones, P. D., T. J. Osborn, and K. R. Briffa, The evolution of climate over the last millennium, *Science*, *292*, 662–667, 2001.

Kaplan, A., M. Cane, Y. Kushnir, A. Clement, M. Blumenthal, and B. Rajagopalan, Analyses of global sea surface temperature 1856–1991, *J. Geophys. Res.*, *103*, 18,567–18,589, 1998.

Keigwin, L. D., The Little Ice Age and medieval warm period in the Sargasso Sea, *Science*, *274*, 1504–1508, 1996.

Kinsman, D. J. J., and H. D. Holland, The co-precipitation of cations with $CaCO_3$ - IV. The co-precipitation of Sr^{2+} with aragonite between 16° and 96°C, *Geochim. Cosmochim. Acta*, *33*, 1–17, 1969.

Kuhlmann, K., Reproduzierbarkeit stabiler Isotopenwerte in Schwammskeletten, M.S. thesis, Univ. Kiel, 2000.

Lazareth, C. E., P. Willenz, J. Navez, E. Keppens, F. Dehairs, and L. André, Sclerosponges as a new potential recorder of environmental changes: Lead in Ceratoporella nicholsoni, *Geology*, *28*, 515–518, 2000.

Levitus, S., *Climatological Atlas of the World Ocean*, *NOAA Prof. Pap. 13*, U.S. Dept. of Commerce, Washington, D. C., 1982.

Levitus, S., and T. Boyer, *World Ocean Atlas 1994,* vol. 4, *Temperature,NOAA Atlas NESDIS, 4*, U.S. Dept. of Commerce, Washington, D. C., 1994.

Levitus, S., R. Burgett, and T. Boyer, *World Ocean Atlas 1994*, vol. 3, *Salinity*, *NOAA Atlas NESDIS 3*, U.S. Dept. of Commerce, Washington, D. C., 1994.

Levitus, S., J. I. Antonov, T. P. Boyer, and C. Stephens, Warming of the World Ocean, *Science*, *287*, 2225–2229, 2000.

Lough, J. M., and D. J. Barnes, Several centuries of variation in skeletal extension, density and calcification in massive Porites colonies from the Great Barrier Reef: A proxy for seawater temperature and a background of variability against which to identify unnatural change, *J. Exp. Mar. Biol. Ecol.*, *211*, 29–67, 1997.

Mann, M. E., R. S. Bradley, and M. K. Hughes, Global-scale temperature patterns and climate forcing over the past six centuries, *Nature*, *392*, 779–787, 1998.

Mann, M. E., R. S. Bradley, and M. K. Hughes, Northern Hemisphere temperatures during the past millennium: Inferences, uncertainties, and limitations, *Geophys. Res. Lett.*, *26*, 759–762, 1999.

McConnaughey, T. A., J. Burdett, J. F. Whelan, and C. K. Paull, Carbon isotopes in biological carbonates: Respiration and photosynthesis, *Geochim. Cosmochim. Acta*, *61*, 611–622, 1997.

Molinari, R. L., D. A. Mayer, J. F. Festa, and H. F. Bezdek, Multiyear variability in the near-surface temperature structure of the midlatitude western North Atlantic Ocean, *J. Geophys. Res.*, *102*, 3267–3278, 1997.

Moore, M. D., C. D. Charles, J. L. Rubenstone, and R. G. Fairbanks, U/Th-dated sclerosponges from the Indonesian seaway record subsurface adjustments to west Pacific winds, *Paleoceanography*, *15*, 404–416, 2000.

Morrison, J. M., and W. D. Nowlin, General distribution of water masses within the eastern Caribbean Sea during the winter of 1972 and fall of 1973, *J. Geophys. Res.*, *87*, 4207–4229, 1982.

Müller, A., M. K. Gagan, and M. T. McCulloch, Early marine diagenesis in corals and geochemical consequences for paleoceanographic reconstructions, *Geophys. Res. Lett.*, *28*, 4471–4474, 2001.

Müller, A., J. J. G. Reijmer, and S. Roth, Die Kleine Eiszeit an der Großen Bahama Bank, *Schriftenr. Dtsch. Geol. Ges.*, *17*, 144, 2002.

Nadeau, M. J., M. Schleicher, P. M. Grootes, H. Erlenkeuser, A. Gottdang, D. J. W. Mous, J. M. Sarnthein, and H. Willkomm, The Leibniz-Labor AMS facility at the Christian-Albrechts University, Kiel, Germany, *Nucl. Instrum. Methods Phys. Res. B*, *123*, 22–30, 1997.

Press, W. H., B. P. Flannery, S. A. Teukolsky, and W. T. Vetterling, *Numerical Recipes in Pascal: The Art of Scientific Computing*, 759 pp., Cambridge Univ. Press, New York, 1989.

Reitner, J., "Coralline Spongien," Der Versuch einer phylogenetisch-taxonomischen Analyse, *Berliner Geowiss. Abh., Reihe E*, *1*, 1–352, 1992.

Reitner, J., and P. Gautret, Skeletal formation in the modern but ultraconservative chaetetid sponge *Spirastrella* (*Acanthochaetetes*) *wellsi* (Demospongiae, Porifera), *Facies*, *34*, 192–208, 1996.

Roberts, C. M., Connectivity and management of Caribbean coral reefs, *Science*, *278*, 1454–1457, 1997.

Rosenheim, B. E., P. K. Swart, and S. Thorrold, Calibration of Sr/Ca with temperature in sclerosponges, *Eos Trans. AGU*, *82*(49), Fall Meet. Suppl., OS31C-0446, 2001.

Rühlemann, C., S. Mulitza, P. J. Müller, G. Wefer, and R. Zahn, Warming of the tropical Atlantic Ocean and slowdown of thermohaline circulation during the last deglaciation, *Nature*, *402*, 511–514, 1999.

Schmitz, W. J., and M. S. McCartney, On the North Atlantic circulation, *Rev. Geophys.*, *31*, 29–49, 1993.

Schmitz, W. J., and P. L. Richardson, On the sources of the Florida current, *Deep Sea Res.*, *38*, suppl. 1, 379–409, 1991.

Shen, C.-C., T. Lee, C.-Y. Chen, C.-H. Wang, C.-F. Dai, and L.-A. Li, The calibration of D[Sr/Ca] versus sea surface temperature relationship for *Porites* corals, *Geochim. Cosmochim. Acta*, *60*, 3849–3858, 1996.

Shindell, D. T., G. A. Schmidt, M. E. Mann, D. Rind, and A. Waple, Solar forcing of regional climate change during the Maunder minimum, *Science*, *294*, 2149–2152, 2001.

Sprintall, J., and M. Tomczak, Evidence of the barrier layer in the surface layer of the tropics, *J. Geophys. Res.*, *97*, 7305–7316, 1992.

Stott, P. A., S. F. B. Tett, G. S. Jones, M. R. Allen, J. F. B. Mitchell, and G. J. Jenkins, External control of 20th century temperature by natural and anthropogenic forcings, *Science*, *290*, 2133–2137, 2000.

Stuiver, M., and H. A. Polach, Discussion: Reporting of ^{14}C data, *Radiocarbon*, *19*, 355–363, 1977.

Swart, P. K., M. Moore, C. Charles, and F. Böhm, Sclerosponges may hold new keys to marine paleoclimate, *Eos Trans. AGU*, *79*, 636, 638, 1998a.

Swart, P. K., J. L. Rubenstone, C. Charles, and J. Reitner, Sclerosponges: A new proxy indicator of climate: Report from the workshop on the use of sclerosponges as proxy indicators of climate, *NOAA Clim. Global Change Program, Spec. Rep. 12*, 19 pp., NOAA, 1998b.

Swart, P. K., B. E. Rosenheim, S. Thorrold, and J. Rubenstone, Annual variation in the chemical composition of sclerosponges, *Eos Trans. AGU*, *82*(47), Fall Meet. Suppl., F634, 2001.

Swart, P. K., S. Thorrold, B. Rosenheim, A. Eisenhauer, C. G. A. Harrison, M. Grammer, and C. Latkoczy, Intra-annual variation in the stable oxygen and carbon and trace element composition of sclerosponges, *Paleoceanography*, *17*(3), 1045, doi:10.1029/2000PA000622, 2002a.

Swart, P. K., H. Elderfield, and M. J. Greaves, A high-resolution calibration of Sr/Ca thermometry using the Caribbean coral *Montastrea annularis*, *Geochem. Geophys. Geosys.*, *3*(11), 8402, doi:10.1029/2002GC000306, 2002b.

Vauclair, F., and Y. du Penhoat, Interannual variability of the upper layer of the tropical Atlantic Ocean from in situ data between 1979 and 1999, *Clim. Dyn.*, *17*, 527–546, 2001.

Vautard, R., P. Yiou, and M. Ghil, Singular-spectrum analysis: A toolkit for short, noisy chaotic signals, *Phys. D*, *58*, 95–126, 1992.

Veizer, J., and J. Wendt, Mineralogy and chemical composition of recent and fossil skeletons of calcareous sponges, *Neues Jahrb. Geol. Palaeontol. Monatsh., 1976*, 558–573, 1976.

Waple, A. M., M. E. Mann, and R. S. Bradley, Long-term patterns of solar irradiance forcing in model experiments and proxy based surface temperature reconstructions, *Clim. Dyn.*, *18*, 563–578, 2002.

Watanabe, T., A. Winter, and T. Oba, Seasonal changes in sea surface temperature and salinity during the Little Ice Age in the Caribbean Sea deduced from Mg/Ca and $^{18}O/^{16}O$ ratios in corals, *Mar. Geol.*, *173*, 21–35, 2001.

Willenz, P., and W. D. Hartman, Growth and regeneration rates of the calcareous skeleton of the Caribbean coralline sponge *Ceratoporella nicholsoni*: A long term survey, *Mem. Queensland Mus.*, *44*, 675–685, 1999.

Winter, A., H. Ishioroshi, T. Watanabe, T. Oba, and J. Christy, Caribbean sea surface temperatures: Two-to-three degrees cooler than present during the Little Ice Age, *Geophys. Res. Lett.*, *27*, 3365–3368, 2000.

Wörheide, G., The reef cave dwelling ultraconservative coralline demosponge *Astrosclera willeyana* Lister 900 from the Indo-Pacific, *Facies*, *38*, 1–88, 1998.

Wörheide G., P. Gautret, J. Reitner, F. Böhm, M. M. Joachimski, V. Thiel, W. Michaelis, and M. Massault, Basal skeletal formation, role and preservation of intracrystalline organic matrices, and isotopic record in the coralline sponge *Astrosclera willeyana* Lister 1900, in *Proceedings of the 7th International Symposium on Fossil Cnidaria and Porifera*, vol. 1, edited by A. Perejon and J. M. Comas-Rengifo, pp. 355–374, Real Soc. Esp. de Hist. Nat., Madrid, 1997.

Wüst, G., *Stratification and Circulation in the Antillean-Caribbean Basins*, Columbia Univ. Press, New York, 1964.

Zeebe, R. E., An explanation of the effect of seawater carbonate concentration on foraminiferal oxygen isotopes, *Geochim. Cosmochim. Acta*, *63*, 2001–2007, 1999.

Zhong, S., and A. Mucci, Calcite and aragonite precipitation from seawater solutions of various salinities: Precipitation rates and overgrowth compositions, *Chem. Geol.*, *78*, 283–299, 1989.

F. Böhm, W.-C. Dullo, A. Eisenhauer, and A. Haase-Schramm, GEOMAR, Forschungszentrum für Marine Geowissenschaften, Wischhofstr. 1-3, D-24148 Kiel, Germany. (ahaase@geomar.de; fboehm@geomar.de; aeisenhauer@geomar.de; cdullo@geomar.de)

B. Hansen, Institut für Geologie und Dynamik der Lithosphäre, Goldschmidtstr. 3, D-37077 Göttingen, Germany. (bhansen@gwdg.de)

M. M. Joachimski, Institut für Geologie, Universität Erlangen, Schlossgarten 5, D-91054 Erlangen, Germany. (joachimski@geol.unierlangen.de)

J. Reitner, Geobiologie, Geowissenschaftliches Zentrum Göttingen GZG, Goldschmidtstr. 3, D-37077 Göttingen, Germany. (jreitne@gwdg.de)